The Gated Narrow Escape Time for molecular signaling

Jürgen Reingruber and David Holcman

Department of Computational Biology, Ecole Normale Supérieure, 46 rue d'Ulm 75005 Paris, France.

The mean time for a diffusing ligand to activate a target protein located on the surface of a microdomain can regulate cellular signaling. When the ligand switches between various states induced by chemical interactions or conformational changes, while target activation occurs in only one state, this activation time is affected. We investigate this dynamics using new equations for the sojourn times spent in each state. For two states, we obtain exact solutions in dimension one, and asymptotic ones confirmed by Brownian simulations in dimension 3. We find that the activation time is quite sensitive to changes of the switching rates, which can be used to modulate signaling. Interestingly, our analysis reveals that activation can be fast although the ligand spends most of the time 'hidden' in the non-activating state. Finally, we obtain a new formula for the narrow escape time in the presence of switching.

Cellular chemical reactions depend on the activation of small targets by diffusing ligands. This process can be regulated by several parameters such as the geometry of the cellular microdomain, the target shape, or the state of the target and ligand upon encounter. In the past, the activation rate and survival probability of the target were studied for diffusion-influenced chemical reactions where the reactivities of the target or the ligands stochastically fluctuate in time [1, 2, 3]. Interestingly, for slow gating dynamics it was found that both processes are not equivalent, and, for example, a gated target may lead to non exponential behaviour at short times [1, 4, 5, 6]. When the target has a fluctuating potential barrier, there is an optimal combination of parameters for which the mean activation time is minimal, leading to a resonant-like phenomena [7, 8]. In cellular microdomains, target activation may depend on the state of the ligand. This is for example the case in the cytoplasm, where enzymes can switch between an inactive and active state, or in the nucleus, where a transcription factor needs to be first activated in order to bind to a specific DNA promoter [9, 10]. Recently, intermittent search scenarios were introduced and extensively analyzed for a dynamics switching stochastically between fast ballistic phases and slow diffusive phases, while the target can only be found in the diffusing phase [11, 12, 13]: interestingly, switching can decrease the search time, and there are optimal search strategies that minimizes the search time.

In the absence of switching, target activation is determined by the narrow escape time (NET), which is the mean time for a Brownian ligand to find a small target in a confined environment [14, 15, 16, 17, 18]. The NET has been used to compute the mean and variance of chemical reactions with few molecules diffusing in microdomains [19], to estimate the probability and the arrival time of viral particles to nuclear pores [20], or to study the early steps of phototransduction in rod photoreceptor [21].

We study in this letter the gated narrow escape time (GNET) to exit the domain Ω through a small window, if a diffusing ligand stochastically switches between two states 1 and 2 with diffusion coefficients D_1 and D_2, and can exit only in state 1. Switching may be due to conformational changes or chemical interactions. We estimate the GNET using new equations for the sojourn times the ligand spends in the different states. We find that switching not only affects drastically the exit time and the sojourn times, but also, only for $D_2 > D_1$ the GNET can be optimized as a function of the switching rates. In addition, a ligand may exit almost as fast as possible, although it spends most of the time in state 2. Finally, we give a new formula for the GNET in dimension three, which extends the NET formula to the switching case. We also discuss briefly possible applications in cellular signaling.

A Brownian ligand diffuses in a confined domain Ω while switching between states 1 and 2 with Poissonian rate constants k_{12} and k_{21} and diffusion constants D_1 and D_2. Upon encounter, the ligand activates the target located on the small boundary portion $\partial\Omega_a$ only in state 1, while it is reflected otherwise everywhere on the boundary. To study the GNET, we consider the mean sojourn times $u_n(\boldsymbol{x}, m)$ the ligand spends in state n before exiting, conditioned on starting at position $\boldsymbol{x}$ in state m. From the backward Chapman-Kolmogorov equation [22, 23] we find that the $u_n(\boldsymbol{x}, m)$ satisfy the coupled system of equations

$$L_m^* u_n(\boldsymbol{x}, m) - \sum_{i=1}^{2} k_{mi}(u_n(\boldsymbol{x}, m) - u_n(\boldsymbol{x}, i)) = -\delta_{nm}, \tag{1}$$

where L_m^* is the backward Kolmogorov operator in state m, which in our case is $L_m^* = D_m\Delta$, and we have absorbing boundary conditions on $\partial\Omega_a$ for $u_n(\boldsymbol{x}, 1)$, and reflecting conditions otherwise. Eq. 1 separately constitutes a closed system of equations for each value n, and it is sufficient to study the equations for $n = 1$, because the solutions $u_2(\boldsymbol{x}, m)$ are obtained through the linear transformation

$$\begin{pmatrix} u_2(\boldsymbol{x}, 1) \\ u_2(\boldsymbol{x}, 2) \end{pmatrix} = \frac{k_{12}}{k_{21}} \begin{pmatrix} 1 & 0 \\ 0 & 1 \end{pmatrix} \begin{pmatrix} u_1(\boldsymbol{x}, 1) \\ u_1(\boldsymbol{x}, 2) \end{pmatrix} + \begin{pmatrix} 0 \\ k_{21}^{-1} \end{pmatrix}. \tag{2}$$
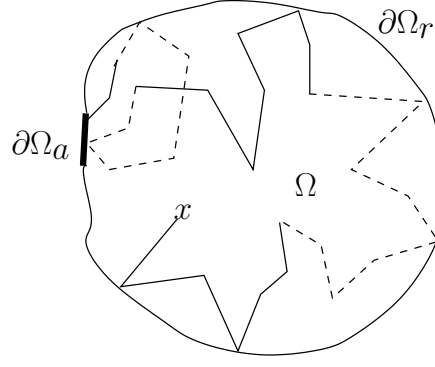
FIG. 1: Example of a trajectory of a diffusing Brownian ligand in a confined domain Ω and randomly switching between two states 1 (continuous line) and 2 (dashed line). In state 2, the ligand is reflected all over the boundary, while in state 1 it is absorbed at $\partial\Omega_a$.

The mean sojourn times $u_1(1)$, $u_1(2)$, $u_2(1)$ and $u_2(2)$ are obtained by averaging eq. 1 and eq. 2 over an initially uniform distribution, satisfying $u_1(2) = u_1(1)$, $u_2(1) = u_1(1)k_{12}/k_{21}$ and $u_2(2) = u_2(1) + 1/k_{21}$. The mean times $u(1)$, $u(2)$ and u to exit the domain starting uniformly distributed in state 1, 2, and in state 1 and 2 with equilibrium probability $(p_1, p_2) = (\frac{k_{21}}{k_{12}+k_{21}}, \frac{k_{12}}{k_{12}+k_{21}})$, are

$$u(1) = u_1(1) + u_2(1) = u_1(1)\left(1 + k_{12}/k_{21}\right) \tag{3}$$

$$u(2) = u_1(2) + u_2(2) = u(1) + 1/k_{21} \tag{4}$$

$$u = p_1 u(1) + p_2 u(2) = u(1) + \frac{k_{12}}{k_{21}(k_{12}+k_{21})} . \tag{5}$$

The GNET in one dimension

We now solve the GNET problem in one dimension where Ω reduces to the interval $0 \leq x \leq L$ with an absorbing boundary at $x = 0$ in state 1, and a reflecting boundary at $x = L$. The one-dimensional analysis already reveals many features that remain valid also in higher dimensions where only asymptotic results are available. Using the scaled parameters

$$l_1 = k_{12}L^2/D_1 , \quad l_2 = k_{21}L^2/D_2 , \quad \kappa = D_1/D_2 \tag{6}$$

we solve eq. 1 and eventually obtain

$$
\begin{aligned}
u_1(x, 1) &= \frac{L^2}{D_1} \frac{l_1 \left(\cosh\sqrt{l_1+l_2} - \cosh(\sqrt{l_1+l_2}\frac{L-x}{L})\right)}{(l_1+l_2)\sqrt{l_1+l_2}\sinh\sqrt{l_1+l_2}} \\
&\quad + \frac{l_2}{l_1+l_2}\frac{(2L-x)x}{2D_1} ,
\end{aligned}
\tag{7}
$$

from which we derive for the averaged sojourn time

$$u_1(1) = \tau_1 - \frac{l_1}{l_1+l_2}\left(\tau_1 - \frac{L^2}{D_1}f(l_1+l_2)\right) , \tag{8}$$

where $\tau_1 = L^2/(3D_1)$ is the mean first passage time to exit in state 1 without switching, and $f(x) = \frac{\coth\sqrt{x}}{\sqrt{x}} - \frac{1}{x}$ is monotonically decreasing from $1/3$ at $x = 0$ towards 0 for $x \to \infty$. In fig. 2, we plot $u_1(1)$ as a function of l_1 and l_2. Interestingly, because $u_1(1) \leq \tau_1$, we found the non-intuitive result that the sojourn time the ligand spends in state 1 before exiting is always smaller than the mean first passage time τ_1 to exit in this state without switching. Even more surprising, $u_1(1)$ can become arbitrarily small by increasing l_1 (resp. the switching rate k_{12}). This behavior can be understood as follows (see also [3]): for a ligand that starts uniformly distributed in state 1, the probability to find it in the neighborhood of the absorbing boundary at $x = 0$ decreases quickly. But, in state 2 the probability distribution is re-homogenized and after switching back to state 1, the density around $x = 0$ is higher compared to the non-switching case leading to a faster exit. Because the sojourn time $u_1(1)$ can be arbitrarily small, we wonder
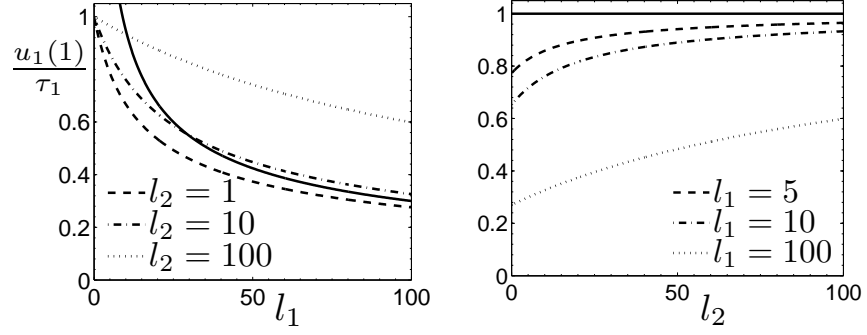
FIG. 2: Graph of the sojourn time $u_1(1)$ obtained from eq. 8 as a function of l_1 and l_2, scaled by the mean first passage time τ_1. In the left panel, the continuous curve is the asymptotic $3/\sqrt{l_1}$ for $l_1 \gg 1$ and $\sqrt{l_1} \gg l_2$.

how this affects the mean time $u(1)$ to exit when starting initially in state 1. Using eq. 8 we obtain

$$u(1) = \tau_1 + \frac{l_1}{l_2}\left(\frac{L^2}{D_1}f(l_1 + l_2) + (\kappa - 1)u_1(1)\right), \qquad (9)$$

which shows that $u(1) \geq \tau_1$ for $\kappa \geq 1$. Obviously, by switching to a state with a smaller diffusion constant, we cannot speed up exit. However, when $\kappa < 1$, interestingly, the situation changes: for fixed l_2, by expanding $u(1)$ in eq. 9 as a function of l_1 for $l_1 \ll 1$, we find that $u(1)$ initially decreases if $l_2 > \tilde{l}_2(\kappa)$, where $\tilde{l}_2(\kappa)$ is the root of $f(l_2) + (\kappa - 1)/3 = 0$. Together with the asymptotic $u(1) \sim \sqrt{l_1}$ for large l_1, we conclude that $u(1)$ has a minimum $u(1)_m < \tau_1$ as a function of l_1 for $l_2 > \tilde{l}_2(\kappa)$. Similar to the results of [11], we found here that the exit time $u(1)$ is minimal for a certain value of k_{12} (that depends on l_2 and κ). The left panel of fig 3 shows $u(1)$ as a function of l_1 for various l_2, and the right panel displays $u(1)$ as a function of l_2 for various l_1, showing that $u(1)$ also has a minimum as a function of l_2. For given values l_2 and $\kappa < 1$, we now study the minimum $u(1)_m$ of $u(1)$ achieved at $l_1 = l_{1,m}$.
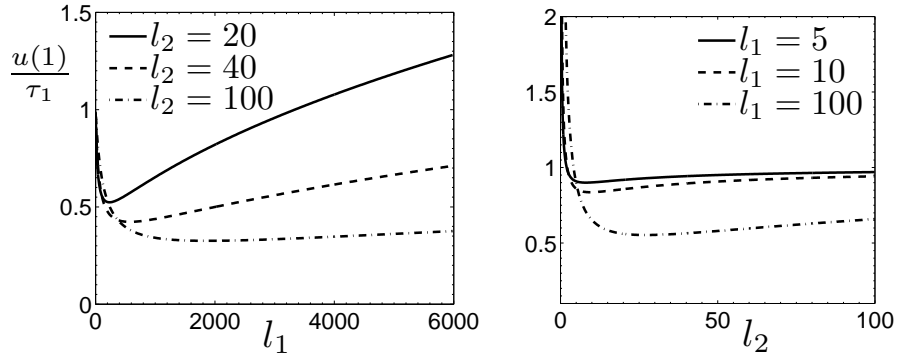

FIG. 3: Graph of the exit time $u(1)$ from eq. 9 as a function of l_1 and l_2 for $\kappa = 0.1$, scaled by τ_1.

The left panel of fig. 4 shows $u_{1,m}$ scaled by τ_1 as a function of l_2 for various κ ($l_{1,m}$ is found by numerically solving $\partial u(1)/\partial l_1 = 0$). An asymptotic analysis for large l_2 reveals that the position $(l_{1,m}, l_2)$ of the minimum is defined by

$$\frac{l_2^2}{l_{1,m}^{3/2}} = \frac{3\kappa}{2(1 - \kappa)}, \qquad (10)$$

from which we derive for large l_2 the asymptotic behaviour $u_1(1)_m = O(l_2^{-1/3})$, $u_2(1)_m = \tau_2 + O(l_2^{-1/3})$ and $u(1)_m = \tau_2 + O(l_2^{-1/3})$, where $\tau_2 = \kappa\tau_1$ is the mean first passage time for a ligand diffusing with a diffusion constant D_2. The right panel of fig. 4 displays the ratio $u_1(1)_m/\tau_1$ and $u_2(2)_m/\tau_2$ as a function of l_2 for different κ. Surprisingly, when exit is fast and $u(1)$ approaches its lower limit τ_2, the ligand spends almost all its lifetime in state 2 where it cannot exit. When considering $u(1)$ as a function of l_2 for a given value of l_1, the minimum position $(l_1, l_{2,m})$ differs from $(l_{1,m}, l_2)$, however, it satisfies a very similar relation compared to eq. 10. In general, for $\kappa < 1$, $u(1)$ has no local minimum as a function of (l_1, l_2), but is lower bounded by τ_2. Only for $\kappa \geq 1$ we have the global minimum

$u(1)_m = \tau_1$ trivially attained for $l_1 = 0$ when the ligand does not switch and stays in state 1. Furthermore, for $\kappa = 1$ there is a strategy to exit in almost minimal time τ_1 while spending most of the time hidden in the state 2 where exit is not possible. With $\alpha \ll 1$, the strategy is to choose $\alpha\sqrt{l_1} \gg 1$ and $l_2 = \alpha l_1$ such that $u(1) \approx \tau_1$, and since $u_1(1)/u_2(1) = \alpha$, it follows that the ligand spends only the small fraction $\alpha/(1 + \alpha)$ of its time in state 1.

In summary, the lower limit of $u(1)$ corresponds to a ligand diffusing all the time with the maximal diffusion constant, and interestingly, fast exit can be achieved even when diffusing most of the time in the state where exit is not possible. Furthermore, for $\kappa < 1$, $u(1)$ has a minimum as a function of l_1 resp. l_2 for non-vanishing switching rates, however, as shown in figure 3, the graph for $u(1)$ around and past the minimum is quite flat, while it decays steeply for small switching rates. Thus, the behaviour at small rates is an efficient mechanism to modulate the activation time, and thus cellular signaling.
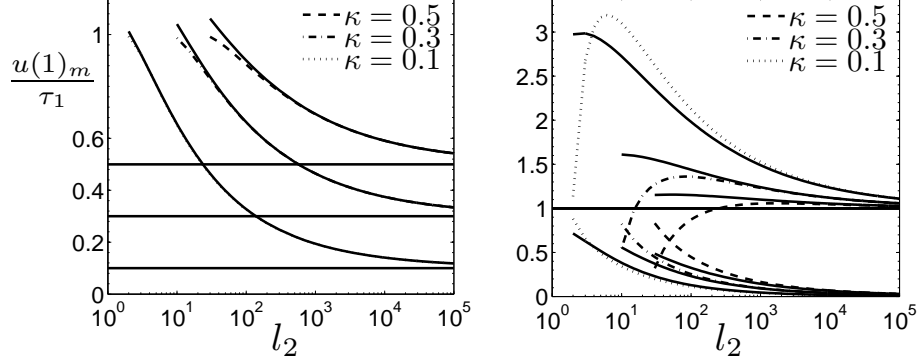

FIG. 4: The left panel displays the minimum $u(1)_m$ scaled by τ_1 as a function of l_2 and κ. The horizontal lines are κ, and the continuous curves are calculated using eq. 10. The graphs do not extend up to $l_2 = 0$ because a minimum exists only for $l_2 > \tilde{l}_2(\kappa)$ (see text). The right panel shows the ratio $u_1(1)_m/\tau_1$ (curves below the horizontal line) and $u_2(1)_m/\tau_2$ (curves above) of the corresponding sojourn times. The continuous curves are calculated using eq. 10.

The GNET in a 3-dimensional microdomain

We now extend our previous analysis to a ligand confined in a 3-dimensional domain Ω that activates upon hitting a small boundary patch $\partial\Omega_a$ in state 1. Without switching, the time reduces to the narrow escape time (NET) [15, 16, 17]. The NET analysis showed that outside a small boundary layer around the absorbing hole of radius a few a, where a characterizes the extent of $\partial\Omega_a$, the positional NET is almost independent of the initial ligand position [17]. Using the scaling introduced in [24], we define the dimensionless variables and functions $\hat{\boldsymbol{x}} = \boldsymbol{x}/a$, $l_1 = k_{12}a^2/D_1$, $l_2 = k_{21}a^2/D_2$, $v_1(\hat{\boldsymbol{x}}) = \frac{aD_1}{|\Omega|}u_1(\boldsymbol{x}, 1)$, $v_2(\hat{\boldsymbol{x}}) = \frac{aD_1}{|\Omega|}u_1(\boldsymbol{x}, 2)$, and obtain from eq. 1 the scaled equations

$$\begin{aligned} \Delta v_1(\hat{\boldsymbol{x}}) - l_1(v_1(\hat{\boldsymbol{x}}) - v_2(\hat{\boldsymbol{x}})) &= -|\hat{\Omega}|^{-1} \\ \Delta v_2(\hat{\boldsymbol{x}}) + l_2(v_1(\hat{\boldsymbol{x}}) - v_2(\hat{\boldsymbol{x}})) &= 0 \,, \end{aligned} \tag{11}$$

where $|\hat{\Omega}| = |\Omega|/a^3 \gg 1$. The boundary conditions are absorbing on $\partial\hat{\Omega}_a$ for $v_1(\hat{\boldsymbol{x}})$, and otherwise reflecting. The solutions of eq. 11 for general values l_1 and l_2 are not at hand, thus we present here asymptotical results that clarify the effect of switching. For $l_1 \ll 1$ or $l_2 \gg l_1$, at leading orders, $v_1(\hat{\boldsymbol{x}})$ is solution of the NET problem $\Delta v_1(\hat{\boldsymbol{x}}) = -|\hat{\Omega}|^{-1}$. When $l_2 \ll \sqrt{l_1}$, the leading order solution for $v_1(\hat{\boldsymbol{x}})$ is found by solving $\Delta v_1(\hat{\boldsymbol{x}}) - l_1(v_1(\hat{\boldsymbol{x}}) - \overline{v_1}) = -|\hat{\Omega}|^{-1}$, where $\overline{v_1}$ is the spatial average of $v_1(\hat{\boldsymbol{x}})$. Using the asymptotic solutions for $v_1(\hat{\boldsymbol{x}})$, the leading order expression of the sojourn time $u(1) = (1 + k_{12}/k_{21})\frac{|\Omega|}{aD_1}\overline{v_1}$ is

$$u(1) = \left(1 + \frac{k_{12}}{k_{21}}\right) \begin{cases} \tau_1, & l_1 \ll 1 \text{ or } l_2 \gg l_1 \\ \dfrac{|\Omega|}{|\partial\Omega_a|\sqrt{D_1 k_{12}}}, & l_1 \gg 1, \sqrt{l_1} \gg l_2 \,. \end{cases} \tag{12}$$

To confirm the behavior of $u(1)$ and $u_1(1)$ as a function of l_1 and l_2, we used Brownian simulations together with the Gillespie-algorithm [25] to model switching in a sphere of radius $r = 30$ with a circular hole of radius $a = 1$. In the left panel of fig. 5, we show simulation results for $u_1(1)$ as a function of l_1 for various l_2. We obtain that $u_1(1) \le \tau_1$, and confirm the asymptotical behaviour $u_1(1)/\tau_1 \approx 4/(\pi\sqrt{l_1})$ which follows from eq. 12 by using $\tau_1 \approx |\Omega|/(4aD_1)$ [18] and $|\partial\Omega_a| = \pi a^2$. In the left panel of fig. 5 we display the simulations results for $u(1)$ as a function of l_1 for various l_2 and $\kappa = 0.1$ ($D_1 = 1, D_2 = 10$). The plot shows that $u(1)$ has a minimum smaller than τ_1 which is attained at some value $l_{1,min} > 0$. For $\kappa \ge 1$, we have $u(1) \ge \tau_1$ (not shown).

The asymptotic expressions in eq. 12 correspond to two different physical regimes (see also the regimes discussed in [3]): In the range where $u_1(1) \approx \tau_1$, the GNET is the NET τ_1 divided by the probability $p_1 = \frac{k_{21}}{k_{12}+k_{21}}$ to find the ligand in state 1, which indicates a mean-field situation where switching and absorption proceed independently. In this range the switching dynamics can be approximated by an effective non-switching diffusion process with diffusion constant $D_{eff} = D_1/p_1$. In the case of $\sqrt{l_1} \gg l_2, l_1 \gg 1$, $u(1)$ and $u_1(1)$ are inversely proportional to the surface of the target, similar to the reaction-controlled NET to a partially absorbing hole [3, 24]. This is very different from the mean-field situation and indicates the appearance of strong correlations.
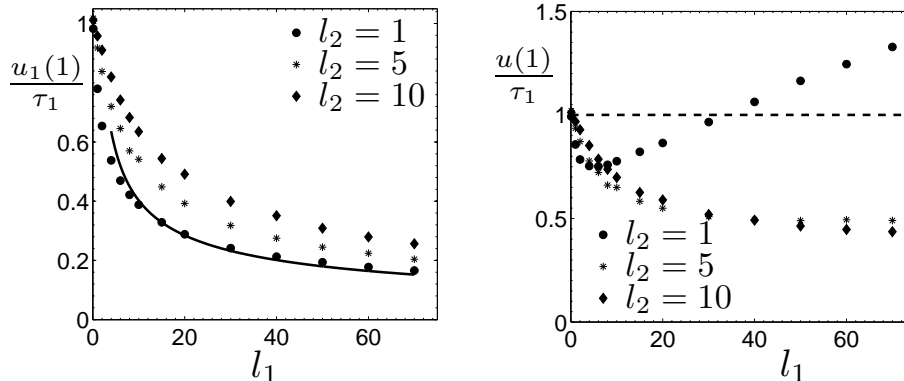

FIG. 5: Simulation results for the sojourn time $u_1(1)$ and the exit time $u(1)$ as a function of l_1 for different l_2 (marked by various symbols). The results are scaled by the NET τ_1. The continuous line in the left panel is the asymptotic $\frac{4}{\pi \sqrt{l_1}}$ obtained from eq. 12 (see also text). The results for $u(1)$ in the right panel are obtained for $\kappa = 0.1$.

To conclude this study of the mean time to activate a target by a switching Brownian ligand, we found the new formula eq. 12 extending the NET to the case of switching. For $D_2 > D_1$, switching can significantly decrease the exit time compared to non-switching. For small values of l_1 and l_2, the mean exit time is very sensitive to changes in these parameters (see fig. 5 and fig. 3), and this property can be exploited to modulate cellular signaling. For example, if switching is due to a chemical reaction, the value of l_1 is changed via k_{12} by modulating the concentration of the reaction partner.

We finish by giving two examples in signal transduction where switching might be important. The first is related to the search time for a promoter DNA-site by a transcription factor (TF), which alternates between a 3-dimensional diffusion in the nucleus and one-dimensional diffusion along the DNA [26, 27, 28]. We consider a TF diffusing along the DNA and switching between two states, triggered by stochastic conformational changes of the TF. In state 1, diffusion is slow due to a high affinity for the DNA where the TF carefully scans the DNA base pairs. In state 2, diffusion is much faster, but the TF does not accurately scan the DNA. The search time of this can be much reduced compared to a TF which carefully checks all the DNA base pairs. The second application illustrates our finding that a diffusing ligand can activate a target fast, although it may spend almost all its time in a state where it has no affinity for the target. This is relevant if a ligand needs to activate a target in a state where it is also prone to some degradation. We found that a ligand can largely avoid degradation and still perform fast target activation by switching between two states, such that it spends most of its time in state 2, where it cannot be degraded nor activate the target.

[1] H. Zhou and A. Szabo, J. Phys. Chem. **100**, 2597 (1996).
[2] A. Berezhkovskii, D. Yang, S. Sheu, and S. Lin, Phys Rev E **54**, 4462 (1996).
[3] C. Doering, Lecture Notes in Physics: Stochastic Processes in Physics, Chemistry, and Biology **557**, 316 (2000).
[4] R. Zwanzig, J. Chem. Phys. **97**, 3587 (1992).
[5] A. Szabo, K. Schulten, and Z. Schulten, J. Chem. Phys. **72**, 4350 (1980).
[6] A. Szabo, D. Shoup, S. Northrup, and J. McCammon, J. Chem. Phys. **77**, 4484 (1982).
[7] C. Doering and G. J.C., Phys Rev Lett. **69**, 2318 (1992).
[8] M. Bier and R. Astumian, Phys Rev Lett. **71**, 1649 (1993).
[9] M. Ptashne, *Genetic Switch: Phage Lambda Revisited* (Cold Spring Harbor, New York, 2004).
[10] C. Barrandon, B. Spiluttini, and O. Bensaude, Biol Cell. **100**, 83 (2008).
[11] O. Bénichou, M. Coppey, M. Moreau, P. Suet, and R. Voituriez, Phys. Rev. Lett. **94**, 198101 (2005).

[12] O. Bénichou, M. Coppey, M. Moreau, P. Suet, and R. Voituriez, J. Phys.-Cond. Mat. **17**, 4275 (2005).

[13] C. Loverdo, O. Bénichou, M. Moreau, and R. Voituriez, Nature Physics **4**, 134 (2008).

[14] M. Ward and J. Keller, SIAM J. Appl. Math. **53**, 770 (1993).

[15] T. Kolokolnikov, M. Titcombe, and M. Ward, Eur. J. Appl. Math. **16**, 161 (2005).

[16] I. V. Grigoriev, Y. A. Makhnovskii, A. M. Berezhkovskii, and V. Y. Zitserman, J. Chem. Phys. **116**, 9574 (2002).

[17] A. Singer, Z. Schuss, and D. Holcman, J. Stat. Phys. **122**, 491 (2006).

[18] Z. Schuss, A. Singer, and D. Holcman, Proc. Natl. Acad. Sci. USA **104**, 16098 (2007).

[19] D. Holcman and Z. Schuss, J. Chemical Physics **122**, 114710 (2005).

[20] E. Lagache, T. Dauty and D. Holcman, Phys. Rev. E **79**, 011921 (2009).

[21] J. Reingruber and D. Holcman, Phys. Rev. E **79**, 030904 (20089).

[22] Z. Schuss, *Theory and Applications of Stochastic Differential Equations* (Wiley Series in Probability and Statistics, John Wiley Sons, Inc., New York, 1980).

[23] H. Risken, *The Fokker-Planck Equation* (Springer-Verlag New York, LLC, 1996).

[24] J. A. Reingruber, E. Abad, and D. Holcman, J. Chem. Phys. **130**, 094909 (2009).

[25] D. T. Gillespie, J. Comp. Phys. **22**, 403 (1976).

[26] J. Elf, G. Li, and X. Xie, Science **316**, 1191 (2007).

[27] Y. Wang, R. Austin, and E. Cox, Science **97**, 048302 (2007).

[28] P. Von Hippel and B. O.G., J. Biolog. Chemistry **264**, 675 (1989).